[1]Sonia Arora
[2]Gouri Sankar Mishra

Revolutionizing MRI-Based Brain Tumor Classification with BrainMRI-NetX for Superior Accuracy and Reliability

Journal of Electrical Systems

Abstract: - This study aims to enhance and ensure reliable MRI-based brain tumor classification through the development of an innovative BrainMRI-NetX model, incorporating advanced techniques such as Depthwise Separable Convolutions, Residual Blocks, Squeeze-and-Excite Blocks, and Self-Attention Layers. For feature extraction, we utilized a hybrid VGG19 and LSTM model. Our primary goal is to develop and evaluate a CNN model that outperforms state-of-the-art models in terms of F-score, recall, accuracy, and precision. The proposed BrainMRI-NetX model was trained using cutting-edge optimization techniques on a large dataset of FigShare MRI brain images, significantly enhancing its performance. We thoroughly evaluated the model's critical performance indicators: F-score, recall, accuracy, and precision. When benchmarked against popular models such as ResNet-152, DenseNet121, and VGG16, our proposed model demonstrated superior performance, achieving an F-score of 0.96, and recall, accuracy, and precision all at 0.99. In comparison, DenseNet121 showed an accuracy of 0.85, precision of 0.89, recall of 0.90, and F-score of 0.88. ResNet-152 and VGG16 exhibited lower performance metrics, with accuracy at 0.86, precision at 0.85, recall at 0.84, and F-score at 0.87. The exceptional performance of our proposed BrainMRI-NetX model highlights its potential for advancing medical diagnostics, particularly in MRI-based brain tumor classification.

Keywords: BrainMRI-NetX, MRI-based brain tumor classification, CNN, Hybrid VGG19-LSTM model, medical image processing.

1. INTRODUCTION

A complex and sometimes fatal medical issue, brain tumours impact a vast number of individuals across the globe. Better patient outcomes and more efficient treatment are possible only with prompt and accurate detection of brain tumours. Although imaging tools such as CT and MRI provide light on the complex brain's architecture, analysing the data typically requires skilled radiologists, which may be a time-consuming process and introduces the possibility of human error. New developments in machine learning and AI have opened up promising avenues for the development of more precise methods for diagnosing brain tumours. [1]. Enhancing the accuracy of brain cancer identification is the focus of this study, which explores the utilisation of When used in tandem with SVMs, Long Short-Term Memory networks. Diagnosing brain tumours requires a meticulous review of medical images to identify benign from malignant tumours, as well as to localise and categorise them [2]–[6]. The traditional method mainly depends on the visual analysis of imaging data, which might be unreliable due to the differing levels of proficiency across radiologists. In response to these difficulties, there is an increasing fascination with creating automated systems capable of analysing medical images with great accuracy. Machine learning methods have demonstrated considerable potential in this domain, specifically by utilising classification algorithms and deep learning models[7]–[11].

Figure 1 Brain Tumor Detection

[1] * Sonia Arora, Department of Computer Science & Engineering
[2] * Gouri Sankar Mishra, Department of Computer Science & Engineering

When it comes to supervised learning, Support Vector Machines (SVMs) see heavy use for tasks like regression and classification. When the data does not follow a linear pattern, Support Vector Machines (SVMs) excel because of their ability to handle multi-dimensional data. Support vector machines (SVMs) may classify MRI images as either benign or malignant, or as having a tumour. This classification can help in the identification of brain cancer. Finding the best hyperplane in the feature space for class separation is crucial for Support Vector Machines (SVMs) to perform their task. This is a first step towards developing a trustworthy approach to tumour classification using picture data. Among the RNN subset, LSTM networks excel at learning and remembering associations between fresh data sets. Many fields make use of long short-term memory (LSTMs), such as time series analytics and natural language understanding. With their exceptional sensitivity, they prove to be an invaluable asset within the realm of tracking medical imaging sequences. Using past data from previous tumour growth predictions or obtaining new data from a series of magnetic resonance imaging (MRI) scans is one way in which LSTMs outperform previous approaches for detecting brain tumours.

[12]–[16].
Using a hybrid strategy that incorporates both SVMs and LSTM networks, this study presents a new multimodal approach to enhancing brain tumour identification. The suggested method aims to merge the temporal learning capabilities of LSTM models for sequential data processing with the discriminative power of SVMs for static photo categorisation [17]–[21]. This combination not only improves the precision of cancer detection, but it also offers a more thorough examination of tumour characteristics. Using a mix of support vector machines and extended short-term memories, this study aims to develop a strong foundation for brain tumour identification. It will compare the combined model's performance against current approaches to find out if this multimodal approach to therapy is beneficial. More accurate diagnoses, shorter interpretation times, and a more dependable tool would be available to medical professionals via the proposed method. Improving healthcare solutions requires developing a system that can detect brain tumours efficiently using modern machine learning algorithms. What follows is a suggested blend of This endeavour may lead to advancements in healthcare imaging and the detection of brain tumours by utilising There are two types of support vector machines: SVMs and LSTMs [22]–[26].

1.1 Establishing Context and Significance

Neuroimaging and medical diagnostics face a significant hurdle in the precise identification and categorisation of brain tumours. Manual MRI analysis by radiologists is one example of a traditional method for brain tumour detection; nevertheless, it is labor-intensive and vulnerable to unpredictability because picture interpretation is subjective. New developments in machine learning and artificial intelligence (AI) provide encouraging avenues for improving the efficacy and precision of diagnostics. In order to overcome the shortcomings of conventional procedures, a multimodal strategy combines numerous methodologies [27]–[31].
For better diagnostic results, multimodal techniques combine data from several sources or use multiple algorithms. Brain tumour diagnosis using these methods could involve a mix of neural networks with convolutional layers, learning via transfer, and advanced methods for preparing images. To automate feature extraction, for example, CNNs and other deep learning models can eliminate the need for human intervention and, perhaps, spot small patterns in MRI scans that would otherwise go unnoticed. Potentially improving diagnostic accuracy, decreasing mistake rates, and allowing earlier diagnosis of brain tumours are the key benefits of such a multimodal approach. Better utilisation of medical resources, better treatment planning, and better patient outcomes are all possible results of better diagnostic technologies. By utilising a range of technology innovations, this strategy signifies a major leap forward in the pursuit of accurate and prompt brain tumour diagnosis [32]–[35].

2. LITERATURE REVIEW

Athisayamani 2023 et. al One way to decrease feature size is to use a Python classifier with ResNet-152 and the Figshare dataset. Its 98.85 percent accuracy rate was higher than competitors' when using specificity, accuracy, & sensitivity measurements% [36]. Saeedi 2023 et. al Through the differentiation of benign brain tissue from malignant gliomas and meningiomas, magnetic resonance imaging (MRI) allows for early identification. A training accuracy of 96.47% in an 8-layer 2D convolutional neural network (CNN) outperformed competing methods for cancer classification after analysing 3,264 MRI data [37]. Liu 2023 et. al Brain tumour segmentation is only one area where deep learning has recently demonstrated promising results, along with object identification, semantic segmentation, and picture categorisation. Covering topics like as network topologies, multi-modality

processes, and handling imbalanced data, this review analyses more than 150 publications on recent deep learning methods and provides directions for future research [38].

Pitchai 2023 et. al Manual cancer tissue segmentation is labor-intensive, but future automated models promise quicker, more accurate diagnoses and treatments. This research develops an RCNN-based MRI prognosis system for brain tumors, using a U-Net encoder for feature extraction. Simulation results validate that the model improves accuracy in tumor size estimation and prognosis[13].

Khan 2022 et. al We look at a way to help radiologists find tumours, and we find that deep learning is better than the old ways of diagnosing brain tumours. Using deep learning, this study presents two models for binary and multiclass classification, with respective accuracy rates of up to 97.8% and 100% [15]. [39]

Table.1 Literature Summary

Author/year	Method	Research gap	Controversies	References
Sinha/2024	With 1747 pictures, an AI-driven brain tumour diagnosis programme achieves 92% accuracy.	Investment in computational resources and different datasets for AI brain tumour diagnosis is necessary.	AI models' reliance on diverse data sets and computational resources is a cause for concern.	[40]
Kamsali/2024	The use of MRI, CT, and PET in architecture allows for the accurate diagnosis and classification of brain tumours.	The multi-modal imaging architecture lacks broad datasets and substantial testing.	There are issues about the reliability of dynamic routeing and multi-modal imaging integration.	[41]
Vinod/2024	Brain tumour segmentation achieved 98.28% accuracy using Ensemble U-Net, CNN, and SOFM model.	Automated brain tumour diagnosis requires various datasets and validation in the actual world.	There are questions about the reliability of automated detection and how it is dependent on specific datasets.	[42]
Asiri/2024	A two-module system for accurate brain tumour identification employing MRI, filtering, and support vector machines.	Improving MRI-based approaches requires more extensive validation and standardised classification.	Concerns over the standardisation of methods and the reliability of automated MRI-based tumour detection.	[43]
Zubair/2024	Improved accuracy of MRI-based brain tumour detection by an EffectiveNetB2 AI model.	The necessity of strong AI models applicable to various MRI tumour datasets.	Harmoniousness of AI-powered magnetic resonance imaging tumour identification in diverse clinical contexts.	[44]

3. METHODOLOGY

Brain tumour MRI image categorisation using the proposed methodology is systematic from data collection to model training. In order to ensure that the dataset contains a diverse variety of tumour types and patient demographics, the initial step is to gather MRI scans from many sources. Photo resizing, pixel value normalisation, and augmentation techniques like flipping and rotation are all part of data preparation's efforts to increase a dataset's diversity. After the images are grayscaled to make computations easier, the following step is to encode the labels in order to train the model effectively. Exploratory Data Analysis (EDA) verifies the dataset's balance and class distribution to ensure representativity between the test and training sets. Feature extraction use a VGG19 model with pre-trained weights to understand intricate image properties; temporal feature augmentation, on the other hand, employs Long Short-Term Memory (LSTM) layers to understand sequential patterns. Using softmax activation, the final classification layers sort images into different types of tumours. After building the model with the Adam optimizer and the categorical cross-entropy loss function, we fine-tuned the hyperparameters to achieve the optimal running time. We employ state-of-the-art

techniques such as Residual Blocks and Depthwise Separable Convolutions to improve classification accuracy and address issues like vanishing gradients in order to efficiently process large MRI images.

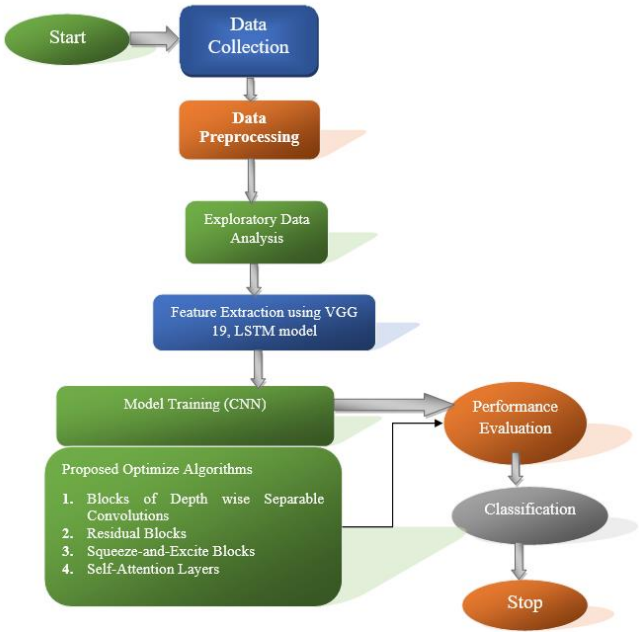

Figure 2 Proposed Flowchart

3.1 Data Collection

Brain tumour data collection To classify magnetic resonance imaging (MRI) images, one must first compile a large collection of these images and then sort them into categories like malignancy, cancer of the pituitary gland, glioma, or no tumour at all. This dataset's diversity includes a wide range of imaging modalities, patient demographics, demographics, and tumour characteristics—is crucial for the successful training of robust models. Publicly available datasets such as figshare, the SARTAJ dataset, and Br35H, as well as medical databases and research collaborations, are common sources for photos. In order to keep the dataset trustworthy, accurate labelling by medical professionals is crucial.All data utilised in this analysis came from publicly available sources [39], ensuring that it meets the required diversity and quality standards for effective brain tumor classification. Proper data preparation and expert labeling are key to developing a reliable and accurate classification model.

3.2 Data Preprocessing

Approaches to data preparation for brain tumour studies A substantial preparing data to train an algorithm for MRI image classification requires a significant amount of time. effectively. First, make sure all of the photos are the same size by resizing them to a standard dimension, like 224 by 224 pixels. The next step was to give each pixel a value between 0 and 1. When data is standardised, the resulting model is more likely to converge. Data augmentation seeks to improve the model by increasing the dataset's diversity. The approaches use image manipulation techniques like zooming, rotating, and flipping to generate a huge dataset of training samples. If the photographs aren't already grayscale, convert them to that mode. This will simplify the input data and reduce computing complexity. For the model to comprehend the classifications during training, it is essential to encode the labels accurately. Preparation procedures such as data augmentation, normalisation, scaling, grayscale conversion, and label encoding are essential for building an ideal and uniform dataset. Our secret weapon for training reliable classification models is thorough data preparation. Brain cancers can be quickly and accurately detected in MRI images with the use of these models. The effectiveness of the picture categorisation job depends on this careful method of data preparation.

Pseudocode for Brain Tumor MRI Image Preprocessing
Define target dimensions for resizing target_width = 224 target_height = 224

```
# Initialize list for preprocessed images and labels
preprocessed_images = []
encoded_labels = []
# Define normalization range
norm_min = 0
norm_max = 1
# Function to resize image
def resize_image(image, width, height):
    # Resize the image to target dimensions
    return resized_image
# Function to normalize pixel values
def normalize_image(image, min_value, max_value):
    # Normalize pixel values to range [min_value, max_value]
    return normalized_image
# Function to apply data augmentation
def augment_image(image):
    # Apply rotation, flipping, and zooming
    return augmented_image
# Function to convert image to grayscale
def convert_to_grayscale(image):
    # Convert the image to grayscale
    return grayscale_image
# Function to encode labels
def encode_label(label):
    # Encode the label appropriately
    return encoded_label
# Loop over all images and labels in the dataset
for image, label in dataset:
    # Resize the image
    resized_image = resize_image(image, target_width, target_height)
    # Normalize the image
    normalized_image = normalize_image(resized_image, norm_min, norm_max)
    # Apply data augmentation
    augmented_image = augment_image(normalized_image)
    # Convert to grayscale if necessary
    if not is_grayscale(augmented_image):
        grayscale_image = convert_to_grayscale(augmented_image)
    else:
        grayscale_image = augmented_image
    # Encode the label
    encoded_label = encode_label(label)
    # Append preprocessed image and label to the lists
    preprocessed_images.append(grayscale_image)
    encoded_labels.append(encoded_label
# Final preprocessed dataset
preprocessed_dataset = (preprocessed_images, encoded_labels)
```

3.3 Exploratory Data Analysis

Brain cancer MRI image classification has made use of a number of exploratory data analysis (EDA) approaches to graphical representation of data insights. In order to fully grasp the dataset's cancer type distribution and variety, we begin by analysing the class samples found in the training photographs. Imparting a balanced representation of each class affects the model's efficiency and is thus a crucial step. After that, check the class to make sure the data used to evaluate the model is accurate and reliable diverse. samples included in the test images. We can find out whether there are any biases or differences between the training and testing samples that could affect the model's generalizability. We use data visualisation techniques to depict the training data's class distribution in order to gain a deeper understanding the dataset. To make sure the dataset isn't biassed, this study highlights the distribution of each tumour type in the training set. The testing data also undergoes a similar visualisation, which sheds light on the evaluation set's class distribution. Finally, conduct a comprehensive study of the dataset's overall balance by evaluating the distribution of the testing and training samples. The classification model's robustness and reliability depend on verifying that the two sets are representative of the same underlying population.

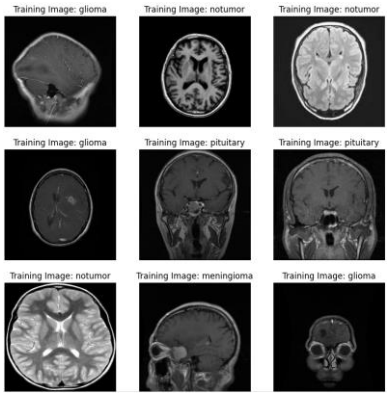

Figure 3 Training Images Class Samples

The image exhibits nine MRI scans, each categorised as a 'Training Image' for glioma, non-tumor, or pituitary problems. These scans are most probably employed for medical education or artificial intelligence training. Each row corresponds to a distinct situation. The convergence of technology and healthcare in enhancing diagnostics is truly captivating. Medical professionals and computational algorithms examine these photos to identify brain tumours and irregularities.

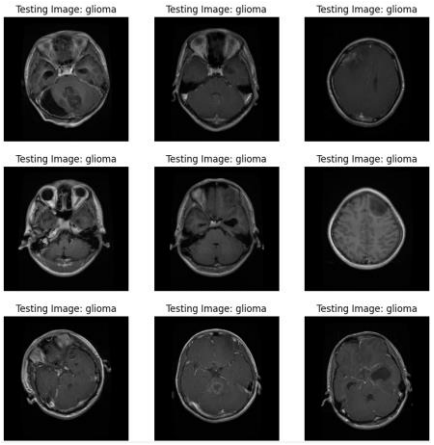

Figure 4 Testing Images Class Samples

The image displays a series of nine monochrome MRI images that are specifically identified as "Testing Image: glioma." These scans are most likely images of different layers of the brain, which help in identifying and analysing gliomas, which are tumours in the brain. The title "Figure 3 Testing Images Class Samples" implies that these images are intended for scientific or instructional purposes. Neurology researchers have a heavy emphasis on gliomas, and these scans are vital for improving diagnostic accuracy and furthering scientific studies.

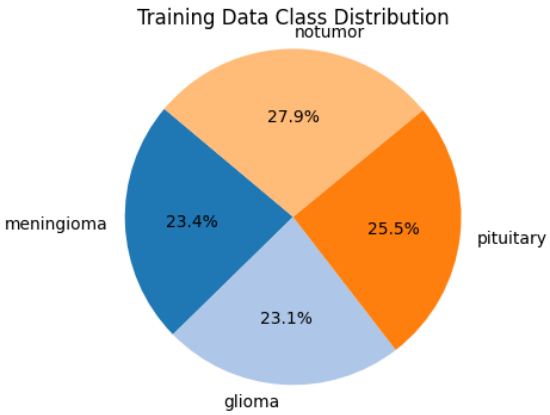

Figure 5 Training Data Class Distribution

The visual representation depicts a pie chart labelled as "Training Data Class Distribution." It depicts the distribution of different brain tumour types in a dataset. The four parts represent the following: meningioma (27.9%), glioma (23.1%), pituitary (25.5%), and absence of a tumour (23.4%). The fairly uniform distribution among these groups is significant for medical research or machine learning applications in healthcare.

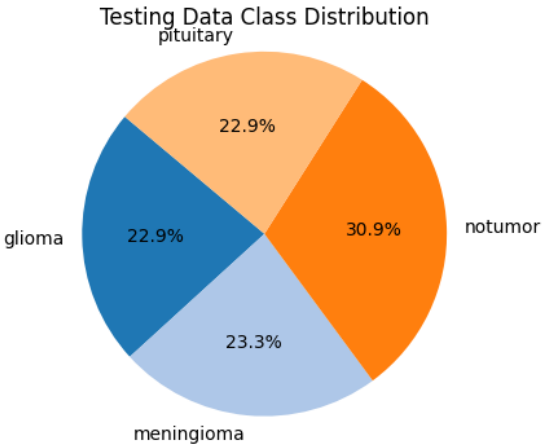

Figure 6 Testing Data Class Distribution

The visual representation depicts a pie chart labelled as "Testing Data Class Distribution." The data is distributed across four categories: glioma, meningioma, notumor, and pituitary. The most significant category is 'notumor' with a proportion of 30.9%, followed by 'glioma' and 'meningioma' both at 22.9%. The tiniest division corresponds to 'pituitary' and accounts for 23.3%. This visualisation is pertinent for the examination of medical data or machine learning jobs where comprehending the proportion of each class is vital.

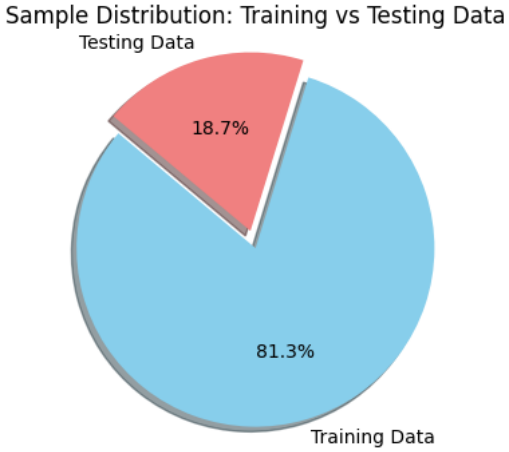

Figure 7 Training and Testing Samples Distribution

The pie graphic depicts data distribution between test and training sets. Approximately 81.3% of the total is training data, and the remaining 18.7% is testing data. This is commonly adopted technique in machine learning ensures that models have the ability to effectively apply learned knowledge to new, unseen data.

3.4 Feature Extraction

Extraction of brain tumour features The capacity to categorise MRI pictures is a crucial component in developing efficient machine learning systems. Using complex deep learning architectures, this method may extract useful information from magnetic resonance imaging (MRI) scans by identifying and capitalising on their complex patterns. Integrating CNNs and RNNs, namely the VGG19 model and LSTM units, is a very effective approach.

- **Initial Feature Extraction using the VGG19 model**

With its pretrained model on the ImageNet dataset, the VGG19 model serves as the primary feature extractor. Its ability to capture fine details in images and its deep architectural design have made this type famous. At the outset of the process, there is an input layer that has been fine-tuned to take pictures with the usual size and colour channels (RGB) (224, 224, 3). Utilising the VGG19 network, this model omits the fully connected top layers. In

order to extract detailed feature maps, VGG19's convolutional layers process the input images. Each block of the convolutional layers has many convolutional layers, and then, to shrink the feature maps, there is a pooling layer. This model can learn and remember a wide variety of abstractions, from simple edges to complex textures and shapes, thanks to its hierarchical structure. Keeping the VGG19 layers unchanged during combined model training helps prevent overfitting and maintains the useful learned properties from the pre-trained model. To make the most of VGG19's powerful feature extraction capabilities during training, the model can keep these layers' weights constant by "freezing" them.

- **Temporal feature enhancement using Long Short-Term Memory (LSTM)**

After VGG19 produces its feature maps, they are downsized such that an LSTM layer can fit inside. One subset of recurrent neural networks (RNNs) developed with the express purpose of capturing and making sense of temporal relationships and patterns LSTM stands for long short-term memory. However, the redesigned feature maps can still reap the benefits of sequential modelling with the help of the LSTM. relationships and improve feature representation, even when MRI scans do not have an inherent temporal aspect. To avoid changing the LSTM layer's weights while training, this approach keeps it in its "non-trainable" state. Because of this, you can be certain that the LSTM layer will only work to enhance the features returned by VGG19 and will not introduce any variability that could lead to overfitting.

- **Last Layers for Classification**

Following processing in the LSTM layer, the output is batch-normalized. This stage involves standardising the output, which decreases the variance in the internal covariate shift and speeds up training. A dense output layer is used to process the normalised output once it is translated into a single vector. The layer uses a softmax function of activation. Classifying photos into four probable diagnoses—glioma, meningioma, hypothalamic tumour, or no tumour at all—is the objective of this thick layer.

Role of LSTM in Feature Extraction

The LSTM layer in the model enhances feature extraction by capturing intricate patterns in the data. Initially, the VGG19 network extracts spatial features from the MRI images. These features are then reshaped into a sequence, which the LSTM processes, identifying significant patterns and relationships within the image. The LSTM's capability to retain and connect information over long sequences allows it to interpret the spatial hierarchy and context of the features. This understanding helps the model retain more detailed information about the image structure. Consequently, the LSTM improves the overall representation of the MRI images, facilitating accurate differentiation between different types of brain tumors.

- **Compilation and Training of the Model**

A model that utilises the Adam optimizer in conjunction with the categorical cross-entropy reduction function; output-oriented. The capacity to modify the learning rate, which enables quicker convergence, and Adam's effectiveness both contribute to its widespread use. Using the categorical cross-entropy loss function with several classes makes it very easy to utilise. It uses a probability value between 0 and 1 to evaluate the performance of a classification model.

The model, its multiple output formats for layers, and the total number of parameters are all visible in the overview. Although there are still numerous trainable factors in the VGG19 model, most of them are frozen. By minimising the LSTM and preserving the remaining thick layers, this model achieves simple and efficient trainable parameters. Properly adjusting the hyperparameters is key to a fruitful training run. We start with a learning rate of 1e-3 and 100 training iterations. Using a 0.95 decay rate for each optimisation step keeps the learning rate from gradually dropping and overshooting. Recall, accuracy, and precision are the three main metrics of our model, which uses categorical cross-entropy as its loss function. Brain tumour strategies that use ANNs and CNNs Classification of magnetic resonance imaging (MRI) images is one possible approach to reliably capturing and applying complicated visual patterns. Our approach ensures accurate and reliable MRI image categorisation by combining LSTM's feature augmentation capabilities with VGG19's initial feature extraction. Medical image analysis involves numerous critical processes; nonetheless, this method stands out due to its thorough preprocessing, model development, and training procedures.

Pseudocode for Feature Extraction using VGG19 and LSTM

```
# Load the VGG19 model without the top layers
vgg19_model = VGG19(weights='imagenet', include_top=False, input_shape=(224, 224, 3))

# Freeze the layers of VGG19 to prevent training
for layer in vgg19_model.layers:
    layer.trainable = False
```

```
# Create the input layer
input_layer = Input(shape=(224, 224, 3))

# Pass the input through the VGG19 model for feature extraction
vgg19_output = vgg19_model(input_layer)

# Reshape the VGG19 output to match the LSTM input dimensions
reshaped_output = Reshape((49, 512))(vgg19_output)

# Define the LSTM layer (non-trainable)
lstm_layer = LSTM(512, trainable=False)(reshaped_output)

# Apply batch normalization
normalized_output = BatchNormalization()(lstm_layer)

# Flatten the output for the final dense layer
flattened_output = Flatten()(normalized_output)

# Add a dense layer with softmax activation for classification (if needed)
output_layer = Dense(4, activation='softmax')(flattened_output)

# Define the feature extraction model
feature_extraction_model = Model(inputs=input_layer, outputs=output_layer)

# Display the model summary
feature_extraction_model.summary()
```

Hyper-Parameter Table:

Hyperparameter	Description	Value
Input Shape	The shape of the input data	(224, 224, 3)
SeparableConv2D Filters	Number of filters in the separable convolution	32
MaxPooling2D Pool Size	Size of the pooling window	(2, 2)
Conv2D Filters	Number of filters in standard convolution	32, 64, 128
Conv2D Kernel Size	Size of the kernel in convolution layers	(3, 3)
Activation Function	Activation function used	ReLU
GlobalAveragePooling2D	Pooling method used	Global Average
Reshape Dimensions	Shape after reshaping layer	(1, 1, X)
Dense Units	Number of units in the dense layers	128, 4
Dropout Rate	Dropout rate for dropout layers	0.5
Number of Heads (Multi-Head Attention)	Number of attention heads	4
Layer Normalization	Whether layer normalization is applied	Yes
Optimizer	Optimization algorithm used	Adam
Learning Rate	Learning rate for the optimizer	0.001
Batch Size	Number of samples per gradient update	32
Epochs	Number of epochs to train the model	100
Loss Function	Loss function used for training	Categorical Crossentropy
Metrics	Metrics to evaluate the model	Accuracy, Precision, Recall

Category cross-entropy loss, the Adam optimisation technique, and the softmax function:

1) Adam Optimization

Adam algorithm draws from momentum and RMSprop optimisation methods. The following is the rule for changing the parameters O in Adam:

$$\theta_{t+1} = \theta_t \frac{\alpha \cdot m_t}{\sqrt{v_t}+\epsilon} \quad (1)$$

2) In the Adam optimisation update rule, the symbols theta, alpha, m t, v t, and epsilon stand for many things. These include the model variables, the learning rate, the squared gradients of past, the exponential decaying averages of past gradients, and a tiny constant that prohibits division by zero.
3) Softmax Function

One method for converting a matrix of initial scores (logits) into probability is by use the softmax function. Here is the definition of the softmax function: when a vector x with K elements is present:

$$Softmax(x)_i = \frac{e^{x_i}}{\sum_{j=1}^{k} e^{x_i}} \quad (2)$$

4) The i-th element of the result vector ({Softmax}(x)i) within the soft max function displays the probability of the appropriate class after each input vector (x) undergoes the softmax transformation.

5) Categorical Cross-Entropy Loss

A popular method for multi-class classification, categorical cross-entropy uses the true distribution (y) and the anticipated distribution to calculate loss:

$$Categorical\ Cross\ Entropy = -\sum_i y_i \cdot \log(\widehat{y_i}) \quad (3)$$

Here, (y_i) denotes the expected distribution of probabilities for the i-th class, and (y_j) displays the actual distribution (one-hot encoded).

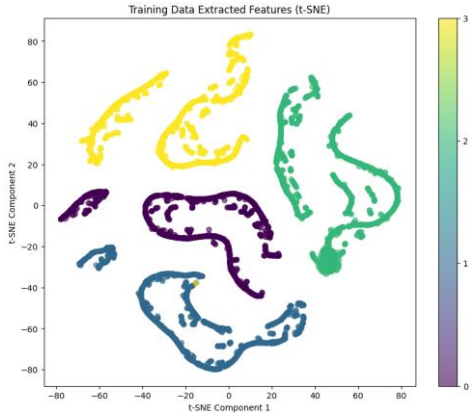

Figure 8 Extracted Features Visualization for training data

The visual representation illustrates a scatter plot of the characteristics of the training data, generated using t-SNE (t-distributed Stochastic Neighbour Embedding). The dataset exhibits distinct categories indicated by clusters of data points in different colours. The axes correspond to the t-SNE components. This visualisation facilitates comprehension of feature extraction and its influence on the training of machine learning models.

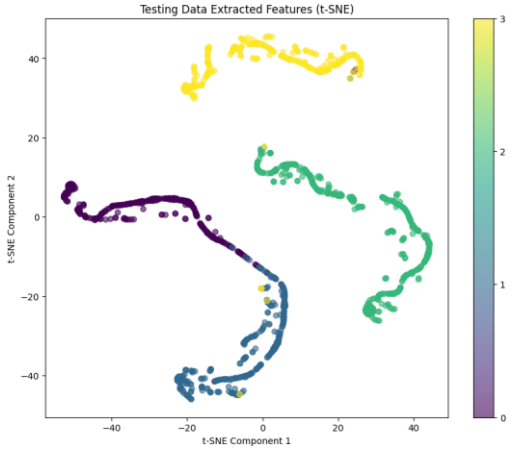

Figure 9 Extracted Features Visualization for testing data

The visual displays a scatter plot labelled "Testing Data Extracted Features (t-SNE). The display exhibits groupings of data points in different hues, symbolising distinct ranges of values. The x-axis is labelled as "t-SNE Component 1," while the y-axis is labelled as "t-SNE Component 2." These clusters expose intrinsic structures within the testing dataset, assisting in comprehending intricate data for tasks such as pattern recognition and classification in machine learning applications.

3.5 BrainMRI-NetX: Advanced CNN Model for Brain Tumor Classification

Our innovative Convolutional Neural Network (CNN) model, BrainMRI-NetX, leverages state-of-the-art optimization algorithms to revolutionize brain tumor classification from MRI images. This cutting-edge deep learning architecture is meticulously designed to enhance feature extraction and ensure highly accurate classification. BrainMRI-NetX effectively handles high-dimensional data and addresses common challenges in deep neural networks. Key components of our model include:

1. Blocks of Depthwise Separable Convolutions

In order to handle big MRI pictures, Depth wise Separable Convolution blocks independently perform both spatial and depth wise convolutions, which dramatically reduces parameters and computing load. In order to effectively filter spatial information while preserving channel integrity, the Depth wise Convolution records spatial correlations inside each channel. Then, information is integrated between channels by the Pointwise Convolution, which makes feature fusion and cross-channel interactions easier. This stage improves the model's comprehension of intricate patterns by honing spatially filtered features. The Depth wise Separable Convolution block accomplishes great representational strength and computational efficiency by splitting these processes; this makes it especially useful in situations where computational resources are few, like in embedded and mobile systems.

- **Depth wise Convolution**

$$Y = \text{DepthwiseConv2D}(X, W_d) \quad (4)$$

Y: output of the convolutional layer with depth.

X: Input feature map.
W_d: Weights of the depth wise convolutional layer.
Regular convolution combines data from several channels by matching input depth with filters. Ideal for mobile applications, depth wise convolution reduces parameters and improves efficiency by forcing feature learning within each channel.

- **Pointwise convolution**

$$Z = \text{Conv2D}(Y, Wp) \quad (5)$$

Z: The pointwise convolutional layer's output.

Y: Output of the depthwise convolutional layer.
Wp: Pointwise convolutional layer weights.

Pointwise convolution uses a 1x1 kernel to integrate information across channels, while depthwise convolution applies separate filters per channel. Combined in depthwise-separable convolution, they enhance efficiency by reducing parameters.

2. Residual Blocks

By utilising skip connections, residual blocks address the disappearing gradient problem, allowing for effective learning in deeper networks and guaranteeing the acquisition of detailed properties. The initial convolutional layer in a Residual block lays the groundwork for later processing by extracting localised patterns and features. Refining these features, the second convolutional layer captures residual information that complements the first. For more refined optimisation while training, the Addition operation merges the initial input with the residual data. By introducing non-linearity, activation functions improve the model's expressive power and performance by enabling it to grasp complicated relationships and depict nuanced patterns within the data.

- First Convolution:

$$Y = \text{Conv2D}(X, W_1) \quad (6)$$

Y: Results from the initial convolutional layer.

X: Input feature map.
W1: Weights of the first convolutional layer.
This layer applies convolution to the input feature map to extract local patterns.

- **Second Convolution:**

$$Z = \text{Conv2D}(Y, W_2) \quad (7)$$

Z: Output of the second convolutional layer.
Y: Output of the first convolutional layer.

W2: Weights of the second convolutional layer.
This layer further processes the features extracted by the first convolutional layer.

- **Addition operation:**

$$A = X + Z \quad (8)$$

A: Combined output.
X: first feature map input (residual connection).

Z: The second convolutional layer's output.

The original input (X) is added to the second convolutional layer's output (Z) in this procedure. A deeper network can learn from its earlier layers by using residual blocks, which enable the network to learn residual mappings.

3. Squeeze-and-Excite Blocks

By strengthening feature map channel connections, the Squeeze-and-Excite (SE) block improves CNN performance. Squeeze, excitation, and scaling are the three operations that make it up. In order to compress global data into channel-wise statistics, the Squeeze operation employs global average pooling. In order to capture complex channel interactions and produce dynamic scaling factors, the Excitation operation uses two convolutional layers. By applying these parameters to feature maps, the Scale operation highlights informative channels while hiding less important ones. Integrating this modular design into CNNs is a game-changer for modern deep learning frameworks since it improves computational efficiency without sacrificing feature discriminative power or the ability to perform tasks like object identification and picture categorisation.

- **Squeeze operation**

$$S_c = \frac{1}{H \times W} \sum_{i=1}^{H} \sum_{j=1}^{W} X_{i,j,c} \quad (9)$$

Xi,j,c refers to the value in channel c from the input feature map at a certain place (i, j).

H discusses the input feature map's height.

W pertains to the input feature map's width.

Sc: This represents the squeezed output for channel c.
Squeeze operation captures the overall significance of a channel by reducing the feature map from its original height x width dimensions to a single value per channel. The next "excitation" procedure uses this channel descriptor to highlight specific informative aspects of the channel.

- **Excitation Operation**

Two convolutional layers are applied to the squeezed representation by the excitation operation in order to capture intricate channel dependencies and produce channel-wise scaling factors.

$$E = \sigma(W_2 \cdot \mathrm{ReLU}(W_1 \cdot S)) \quad (10)$$

σ: Sigmoid activation function.
W2: The second densely connected layer’s weights.

ReLU: ReLU activation function.
W1: The first dense layer’s weights are totally coupled.

S: The output vector that has been squashed.

In order to represent intricate channel relationships and provide scaling factors for each channel, this process makes use of two completely connected layers with activations.

4. Self-Attention Layers

The model's improved contextual understanding and classification performance are a result of the self-attention layers, which enable the model to focus on crucial input elements by capturing their vast interconnections. Based on MRI images labelled as glioma, meningioma, no tumour, or pituitary, this model employs the Adam optimizer for efficient learning and a categorical cross-entropy loss function that is optimal for multi-class classification. Metrics that evaluate the model's reliability and accuracy include F1-score, recall, and precision. Our performance-optimized design is invaluable in medical image processing for dependable and accurate brain tumour diagnosis. The self-attention mechanism enhances the model's ability to concentrate on relevant data while maintaining context using a mix of layer normalisation, multi-head attention, and addition operations. Language modelling and machine translation are two areas that necessitate top-notch performance, and this improves its capacity to comprehend complex patterns and interactions.

- Layer Normalization:

$$X' = \text{LayerNorm}(X) \tag{11}$$

X': Normalized output.
X: Input feature map.
By normalising the input feature map, this guarantees steady training and lessens the model's sensitivity to changes in input magnitude.

- Multi-Head Attention:

$$A = \text{MultiHeadAttention}(Q = X', K = X', V = X') \tag{12}$$

A: Output of the multi-head attention mechanism.
Q: Query matrix (normalized input).
K: Key matrix (normalized input).
V: Value matrix (normalized input).

- Addition Operation:

$$O = X + A \tag{13}$$

O: Combined output.
X: initial feature map input.

A: The multi-head attention mechanism's output.

This increases the multi-head attention mechanism's (A) output by adding the initial input (X). This naturally integrates contextual data from other sequence segments into the feature map.

4. RESULTS AND DISCUSSION

To find out how effectively the Convolutional Neural Network (CNN) Model worked when trained with picture data, optimisation was one of the important evaluation criteria. These numbers tell you a lot about how well the classifier identifies picture classes:

4.1 Accuracy

One way to measure the classifier's accuracy is to divide the total number of guesses by the number of correct predictions.

$$Accuracy = \frac{TP+TN}{TP+TN+FP+FN} \tag{14}$$

4.2 Precision

To measure the classifier's efficacy in spotting critical instances, this statistic compares the total number of plausible but incorrect positive predictions.

$$Precision = \frac{TP}{TP+FP} \tag{15}$$

4.3 Recall (Sensitivity)

How well a classifier finds samples that fit the requirements is called its recall. As a measure of predictive ability, one could look at the ratio of correct to incorrect forecasts.

$$Recall = \frac{TP}{TP+FN} \tag{16}$$

4.4 F1 Score

By combining recall and accuracy, the F1 score gives a comprehensive evaluation of the classifier's performance. Achieving peak efficiency in recall and precision is an enormous feat.

$$F1 - score = \frac{2}{\frac{1}{precision}+\frac{1}{recall}} \tag{17}$$

Table 4.1 Performance Evaluation of Proposed Convolutional Neural Network (CNN) Model

Model	Accuracy	Precision	Recall	F score
Proposed BrainMRI-NetX	0.99	0.99	0.99	0.96

The performance of the proposed BrainMRI-NetX model was assessed using the metrics shown in the table. When tested on several key measures, the model consistently delivers excellent results. With a precision of 0.99, the model's predictions are spot on 99% of the time. The majority of the optimistic forecasts will come true if the

accuracy rate is 0.99. The model properly identifies 99% of the true positive events with a recall of 0.99 as well. When the F-score is 0.96, it means that the statistic considers both recall and precision. Because of this, we know the model can handle datasets with imbalances and still make accurate predictions.

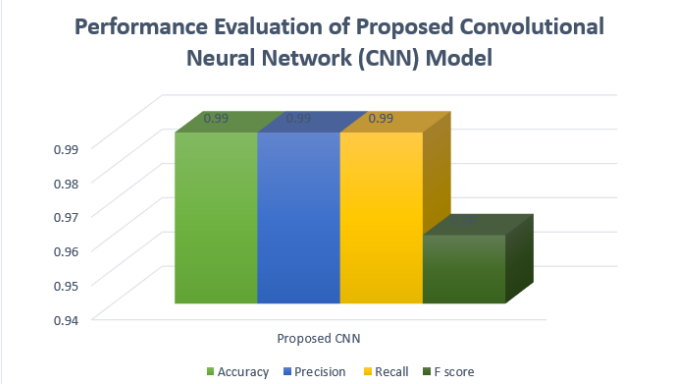

Figure 10 Performance Graph of Proposed Model

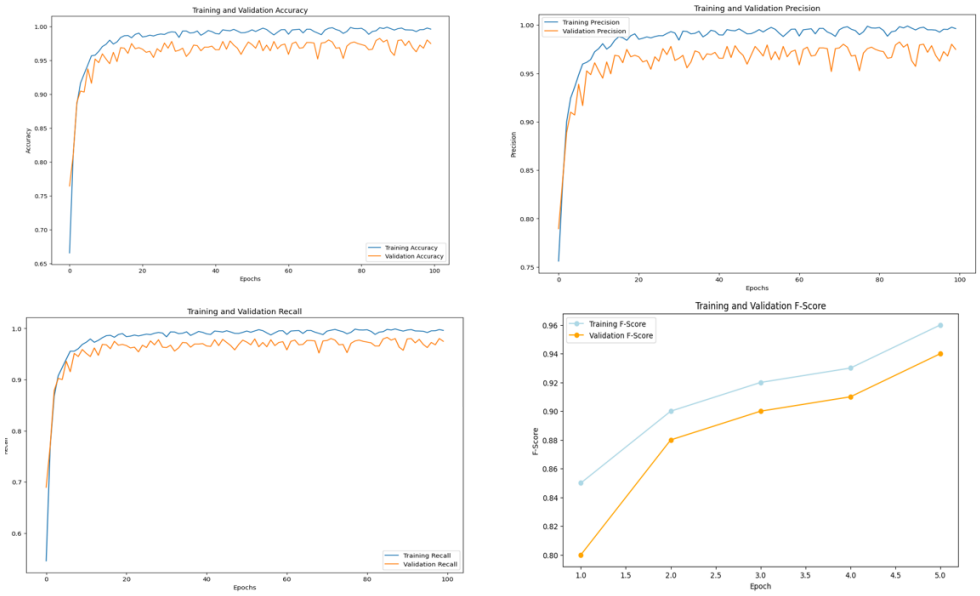

Figure 11 Accuracy Precision Recall and F1 score Graph

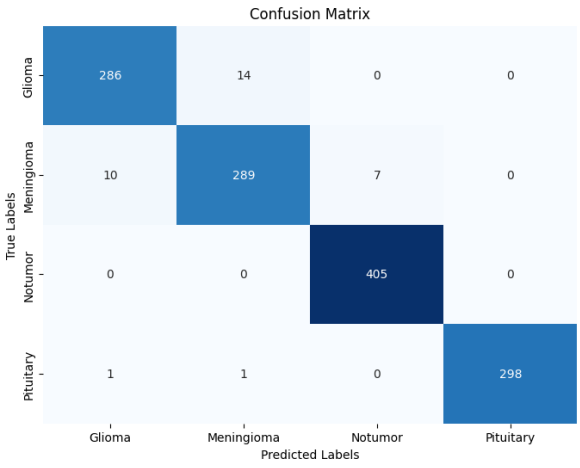

Figure 12 Confusion matrix of proposed model

Table 4.1 Comparative Analysis of Proposed BrainMRI-NetX Model with Optimisation with Existing Models

Model	Accuracy	Precision	Recall	F score	Ref.
Proposed CNN	**0.99**	**0.99**	**0.99**	**0.96**	
Existing Vgg 16	0.86	0.85	0.84	0.87	[45]
Existing DenseNet 121	0.85	0.89	0.90	0.88	[46]
ResNet-152	0.98	0.97	0.95		[36]

In the table, you can see how each generation of Convolutional Neural Networks (CNNs) stacks up against the others. A score of 0.96, accuracy of 0.99, precision of 0.99, and recall of 0.99 indicate that the proposed CNN outperforms the existing models in terms of overall performance. Meanwhile, ResNet-152 (accuracy 0.98, precision 0.97, recall 0.95), DenseNet121 (accuracy 0.85, precision 0.89, recall 0.90, F-score 0.88), and VGG16 (accuracy 0.86, precision 0.85, recall 0.84, F-score 0.87) all show lower scores, despite being successful.

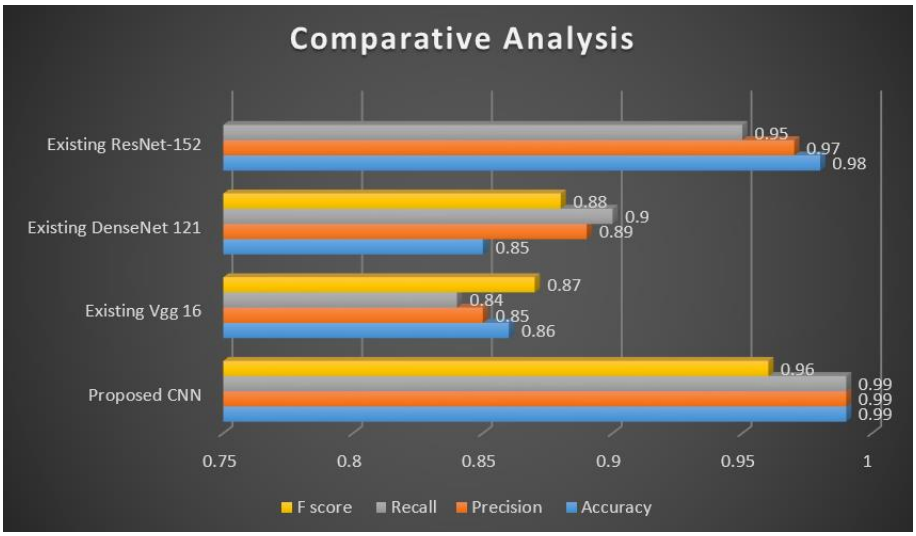

Figure 13 Comparative analysis graph

5. CONCLUSION

This study presents an innovative approach to MRI-based brain tumor classification through the development of the BrainMRI-NetX model, which has demonstrated superior performance in comparison to existing models like VGG16, DenseNet121, and ResNet-152. By achieving an accuracy, precision, and recall of 0.99, along with an F-score of 0.96, the BrainMRI-NetX model sets a new standard for reliability and accuracy in medical image classification. The high performance metrics suggest that this model effectively captures and processes intricate patterns within MRI images, providing a robust solution for the accurate diagnosis of brain tumors. This is of paramount importance in clinical settings, where accurate and early diagnosis is essential for improved patient outcomes.

The rigorous methodology of this study, which includes a comprehensive data preparation process, efficient feature extraction using VGG19, and temporal sequence learning through LSTM, contributes to the model's high effectiveness. Furthermore, the study emphasizes the importance of a well-balanced dataset, enabling the model to generalize across diverse tumor types and patient demographics, making it highly reliable for practical applications. Advanced techniques, including Depthwise Separable Convolutions, Residual Blocks, Squeeze-and-Excite Blocks, and Self-Attention Layers, were integrated to enhance feature learning and address challenges like the vanishing gradient problem, commonly encountered in deep neural networks. Hyperparameter tuning, including the use of the Adam optimizer with a gradual learning rate decay, has also been crucial in optimizing model performance and convergence speed.

The novelty of this research lies in the integration of a hybrid approach that combines VGG19 and LSTM within the BrainMRI-NetX architecture. This fusion brings together the strengths of convolutional neural networks (CNNs) for spatial feature extraction with long short-term memory (LSTM) layers for temporal sequence learning. Unlike traditional CNN-based models, BrainMRI-NetX captures both spatial and sequential patterns, which is critical for analyzing complex brain tumor images with high precision. Additionally, the use of Depthwise Separable Convolutions, Residual Blocks, Squeeze-and-Excite Blocks, and Self-Attention Layers within the model architecture adds further novelty by enhancing feature representation, reducing computational complexity, and improving the model's ability to focus on relevant features.

REFERENCES

[1] Z. Liu, L. Sun, and Q. Zhang, "High Similarity Image Recognition and Classification Algorithm Based on Convolutional Neural Network," *Comput. Intell. Neurosci.*, vol. 2022, 2022, doi: 10.1155/2022/2836486.

[2] S. Einy, H. Saygin, H. Hivehch, and Y. Dorostkar Navaei, "Local and Deep Features Based Convolutional Neural Network Frameworks for Brain MRI Anomaly Detection," *Complexity*, vol. 2022, 2022, doi: 10.1155/2022/3081748.

[3] A. Akilandeswari *et al.*, "Automatic Detection and Segmentation of Colorectal Cancer with Deep Residual Convolutional Neural Network," *Evidence-based Complement. Altern. Med.*, vol. 2022, 2022, doi: 10.1155/2022/3415603.

[4] C. Guo and Z. Li, "Automatic Rock Classification Algorithm Based on Ensemble Residual Network and Merged Region Extraction," *Adv. Multimed.*, vol. 2022, 2022, doi: 10.1155/2022/3982892.

[5] R. Zhou, S. Hu, B. Ma, and B. Ma, "Automatic Segmentation of MRI of Brain Tumor Using Deep Convolutional Network," *Biomed Res. Int.*, vol. 2022, 2022, doi: 10.1155/2022/4247631.

[6] A. S. Ladkat *et al.*, "Deep Neural Network-Based Novel Mathematical Model for 3D Brain Tumor Segmentation," *Comput. Intell. Neurosci.*, vol. 2022, 2022, doi: 10.1155/2022/4271711.

[7] S. Saravanan, V. V. Kumar, V. Sarveshwaran, A. Indirajithu, D. Elangovan, and S. M. Allayear, "Computational and Mathematical Methods in Medicine Glioma Brain Tumor Detection and Classification Using Convolutional Neural Network," *Comput. Math. Methods Med.*, vol. 2022, 2022, doi: 10.1155/2022/4380901.

[8] Z. Chen, N. Li, C. Liu, and S. Yan, "Deep Convolutional Neural Network-Based Brain Magnetic Resonance Imaging Applied in Glioma Diagnosis and Tumor Region Identification," *Contrast Media Mol. Imaging*, vol. 2022, 2022, doi: 10.1155/2022/4938587.

[9] J. Arun Pandian and K. Kanchanadevi, "An improved deep convolutional neural network for detecting plant leaf diseases," *Concurr. Comput. Pract. Exp.*, vol. 2022, no. i, 2022, doi: 10.1002/cpe.7357.

[10] Z. Qian, L. Xie, and Y. Xu, "3D Automatic Segmentation of Brain Tumor Based on Deep Neural Network and Multimodal MRI Images," *Emerg. Med. Int.*, vol. 2022, pp. 1–9, 2022, doi: 10.1155/2022/5356069.

[11] Z. Zhu, H. Chen, S. Xie, Y. Hu, and J. Chang, "Classification and Reconstruction of Biomedical Signals Based on Convolutional Neural Network," *Comput. Intell. Neurosci.*, vol. 2022, 2022, doi: 10.1155/2022/6548811.

[12] Y. Feng, J. Li, and X. Zhang, "Research on Segmentation of Brain Tumor in MRI Image Based on Convolutional Neural Network," *Biomed Res. Int.*, vol. 2022, 2022, doi: 10.1155/2022/7911801.

[13] R. Pitchai *et al.*, "Region Convolutional Neural Network for Brain Tumor Segmentation," *Comput. Intell. Neurosci.*, vol. 2022, 2022, doi: 10.1155/2022/8335255.

[14] M. Sethi, S. Ahuja, S. Rani, D. Koundal, A. Zaguia, and W. Enbeyle, "An Exploration: Alzheimer's Disease Classification Based on Convolutional Neural Network," *Biomed Res. Int.*, vol. 2022, 2022, doi: 10.1155/2022/8739960.

[15] M. S. I. Khan *et al.*, "Accurate brain tumor detection using deep convolutional neural network," *Comput. Struct. Biotechnol. J.*, vol. 20, pp. 4733–4745, 2022, doi: 10.1016/j.csbj.2022.08.039.

[16] P. Tiwari *et al.*, "Medical Imaging," vol. 2022, 2022.

[17] I. Hassan, T. Ali, G. Ali, and T. Ali, "Neural Network and Deep Transfer Learning Approach with MR Imaging Brain Tumor Classification using Convolutional Neural Network and Deep Transfer Learning Approach with MR Imaging," 2022.

[18] K. U. Kurukshetra, "Building Efficient Neural Networks For Brain Tumor Detection," vol. 6, no. 11, pp. 222–235, 2022.

[19] F. Alam *et al.*, "Automated Brain Disease Classification using Transfer Learning based Deep Learning Models," *Int. J. Adv. Comput. Sci. Appl.*, vol. 13, no. 9, pp. 941–949, 2022, doi: 10.14569/IJACSA.2022.01309109.

[20] J. Amin, M. Sharif, A. Haldorai, M. Yasmin, and R. S. Nayak, "Brain tumor detection and classification

using machine learning: a comprehensive survey," *Complex Intell. Syst.*, vol. 8, no. 4, pp. 3161–3183, 2022, doi: 10.1007/s40747-021-00563-y.

[21] L. H. Shehab, O. M. Fahmy, S. M. Gasser, and M. S. El-Mahallawy, "An efficient brain tumor image segmentation based on deep residual networks (ResNets)," *J. King Saud Univ. - Eng. Sci.*, vol. 33, no. 6, pp. 404–412, 2021, doi: 10.1016/j.jksues.2020.06.001.

[22] T. Tazin *et al.*, "A Robust and Novel Approach for Brain Tumor Classification Using Convolutional Neural Network," *Comput. Intell. Neurosci.*, vol. 2021, 2021, doi: 10.1155/2021/2392395.

[23] Z. Liu *et al.*, "Deep Learning Based Brain Tumor Segmentation: A Survey," 2021.

[24] S. Gull, S. Akbar, and H. U. Khan, "Automated Detection of Brain Tumor through Magnetic Resonance Images Using Convolutional Neural Network," *Biomed Res. Int.*, vol. 2021, 2021, doi: 10.1155/2021/3365043.

[25] J. Zhang, J. Yang, and M. Zhao, "Automatic Segmentation Algorithm of Magnetic Resonance Image in Diagnosis of Liver Cancer Patients under Deep Convolutional Neural Network," *Sci. Program.*, vol. 2021, 2021, doi: 10.1155/2021/4614234.

[26] H. Lu, "Computer-Aided Diagnosis Research of a Lung Tumor Based on a Deep Convolutional Neural Network and Global Features," *Biomed Res. Int.*, vol. 2021, 2021, doi: 10.1155/2021/5513746.

[27] Y. Jiang, M. Ye, D. Huang, and X. Lu, "AIU-Net: An Efficient Deep Convolutional Neural Network for Brain Tumor Segmentation," *Math. Probl. Eng.*, vol. 2021, 2021, doi: 10.1155/2021/7915706.

[28] Q. Zhong, H. Lei, Q. Chen, and G. Zhou, "A Sleep Stage Classification Algorithm of Wearable System Based on Multiscale Residual Convolutional Neural Network," *J. Sensors*, vol. 2021, 2021, doi: 10.1155/2021/8222721.

[29] M. Nazir, S. Shakil, and K. Khurshid, "Role of deep learning in brain tumor detection and classification (2015 to 2020): A review," *Comput. Med. Imaging Graph.*, vol. 91, p. 101940, 2021, doi: 10.1016/j.compmedimag.2021.101940.

[30] M. F. Rachmadi, M. del C. Valdés-Hernández, S. Makin, J. Wardlaw, and T. Komura, "Automatic spatial estimation of white matter hyperintensities evolution in brain MRI using disease evolution predictor deep neural networks," *Med. Image Anal.*, vol. 63, p. 101712, 2020, doi: 10.1016/j.media.2020.101712.

[31] H. A. Khan, W. Jue, M. Mushtaq, and M. U. Mushtaq, "Brain tumor classification in MRI image using convolutional neural network," *Math. Biosci. Eng.*, vol. 17, no. 5, pp. 6203–6216, 2020, doi: 10.3934/MBE.2020328.

[32] Q. Zheng, M. Yang, X. Tian, N. Jiang, and D. Wang, "A full stage data augmentation method in deep convolutional neural network for natural image classification," *Discret. Dyn. Nat. Soc.*, vol. 2020, 2020, doi: 10.1155/2020/4706576.

[33] K. Almezhghwi and S. Serte, "Improved Classification of White Blood Cells with the Generative Adversarial Network and Deep Convolutional Neural Network," *Comput. Intell. Neurosci.*, vol. 2020, 2020, doi: 10.1155/2020/6490479.

[34] W. Wu *et al.*, "An Intelligent Diagnosis Method of Brain MRI Tumor Segmentation Using Deep Convolutional Neural Network and SVM Algorithm," *Comput. Math. Methods Med.*, vol. 2020, 2020, doi: 10.1155/2020/6789306.

[35] M. Abdel, A. Helmy, and M. Khattab, "U-Net based Deep Convolutional Neural Network Models for Liver Segmentation from CT Scan Images," no. Sep, 2020.

[36] S. Athisayamani, R. S. Antonyswamy, V. Sarveshwaran, M. Almeshari, Y. Alzamil, and V. Ravi, "Feature Extraction Using a Residual Deep Convolutional Neural Network (ResNet-152) and Optimized Feature Dimension Reduction for MRI Brain Tumor Classification," *Diagnostics*, vol. 13, no. 4, 2023, doi: 10.3390/diagnostics13040668.

[37] S. Saeedi, S. Rezayi, H. Keshavarz, and S. R. Niakan Kalhori, "MRI-based brain tumor detection using convolutional deep learning methods and chosen machine learning techniques," *BMC Med. Inform. Decis. Mak.*, vol. 23, no. 1, pp. 1–17, 2023, doi: 10.1186/s12911-023-02114-6.

[38] Z. Liu *et al.*, "Deep learning based brain tumor segmentation: a survey," *Complex Intell. Syst.*, 2022, doi: 10.1007/s40747-022-00815-5.

[39] "Brain Tumor MRI Dataset." https://www.kaggle.com/datasets/masoudnickparvar/brain-tumor-mri-dataset (accessed Jul. 12, 2024).

[40] A. Sinha and T. Kumar, "Enhancing Medical Diagnostics: Integrating AI for precise Brain Tumour Detection," *Procedia Comput. Sci.*, vol. 235, no. 2023, pp. 456–467, 2024, doi: 10.1016/j.procs.2024.04.045.

[41] S. Kamsali, C. K. Indira, Y. P. S. Reddy, and K. Gayathri, "Multi-Modal Deep Learning Architecture for Precise Brain Tumor Detection," vol. 6, pp. 2170–2182, 2024, doi: 10.33472/AFJBS.6.Si2.2024.

[42] D. S. Vinod, S. P. S. Prakash, H. Alsalman, A. Y. Muaad, and M. B. Bin Heyat, "Ensemble Technique for Brain Tumor Patient Survival Prediction," *IEEE Access*, vol. 12, no. February, pp. 19285–19298, 2024, doi: 10.1109/ACCESS.2024.3360086.

[43] A. A. Asiri, T. A. Soomro, A. A. Shah, G. Pogrebna, M. Irfan, and S. Alqahtani, "Optimized Brain Tumor Detection: A Dual-Module Approach for MRI Image Enhancement and Tumor Classification," *IEEE Access*, vol. 12, no. February, pp. 42868–42887, 2024, doi: 10.1109/ACCESS.2024.3379136.

[44] A. M. J. Zubair Rahman *et al.*, "Advanced AI-driven approach for enhanced brain tumor detection from MRI images utilizing EfficientNetB2 with equalization and homomorphic filtering," *BMC Med. Inform. Decis. Mak.*, vol. 24, no. 1, pp. 1–19, 2024, doi: 10.1186/s12911-024-02519-x.

[45] U. Kosare, L. Bitla, S. Sahare, P. Dongre, S. Jogi, and S. Wasnik, *Automatic Brain Tumor Detection and Classification on MRI Images Using Deep Learning Techniques*. 2023. doi: 10.1109/I2CT57861.2023.10126412.

[46] S. Sharma *et al.*, "Deep Learning Model for Automatic Classification and Prediction of Brain Tumor," *J. Sensors*, vol. 2022, 2022, doi: 10.1155/2022/3065656.